Minerals Engineering 154 (2020) 106406

Contents lists available at ScienceDirect

Minerals Engineering

journal homepage: www.elsevier.com/locate/mineng

Recovery of manganese from ferruginous manganese ore using ascorbic acid as reducing agent

Manish Kumar Sinha[a,*], Walter Purcell[a], Willem A. Van Der Westhuizen[b]

[a] Department of Chemistry, University of the Free State, Bloemfontein 9300, South Africa
[b] Department of Geology, University of the Free State, Bloemfontein 9300, South Africa

ARTICLE INFO

Keywords:
Manganese ore
Reductive leaching
Ascorbic acid
Leaching kinetics
Manganese oxide

ABSTRACT

Being a green and mild acid along with remarkably high solubility for several base metals, ascorbic acid has been used as both leaching agent and reducing agent for the recovery of metals from primary and secondary sources. In the present investigation, ascorbic acid was tested as reducing agent in the presence of sulfuric acid for the leaching of manganese from low grade ferruginous manganese ore. The optimization of the leaching conditions has been comprehensively investigated with respect to H_2SO_4 concentration, temperature, pulp density, ascorbic acid dosage and agitation speed. Quantitative leaching of manganese was observed under the following optimized conditions: 1 M H_2SO_4 concentration, 0.070 M ascorbic acid concentration, 70 g/L pulp density, 60 °C leaching temperature, 800 rpm stirring rate and 300 min of reaction time. The leaching kinetic of manganese was evaluated based on the shrinking core model and further validated by SEM and XRD analysis of manganese ores before and after leaching. After further purification of the leach solution, a high purity of 99.95% α-Mn_2O_3 have been synthesized. The present process therefore deals with achieving the effective recovery of value added product from low grade ferruginous manganese ore.

1. Introduction

Manganese plays a strategically important role in various metallurgical industries across the world such as steel production and alloy making. Approximately 90% of worldwide Mn is exploited in desulfurization and strengthening of steel and cast iron while the remaining 10% of Mn are utilized in multiple non-metallurgical applications like batteries, chemicals, electrochemical, foods, and pharmaceuticals (Top, 2019). Generally, high-grade manganese ores are used for direct smelting of ferromanganese alloys. The rapidly growing demand however leads to the serious depletion of high-grade manganese ore. Chinese industrial classifications of manganese ores are categorized by Mn/Fe mass ratio. The manganese ores with a Mn/ Fe mass ratio > 5 are commercial grade Mn-ores whereas ores with low Mn/Fe mass ratio (< 3) are considered as ferruginous manganese ores. These ferruginous ore resources are profusely available all over the world (Liu et al., 2019) and now focus has been shifted to the utilization of these low-grade ores for the recovery of manganese taking account of scarce availability of high-grade ores. As MnO_2, the main content of manganese oxide ore, is insoluble in dilute sulfuric acid and alkaline media, manganese extraction must be performed under reducing conditions to convert the insoluble Mn(IV) to soluble Mn(II) in aqueous medium. The typical process of hydrometallurgy applied different reducing agents for the recovery of manganese from variety of ores. The reductive leaching of Mn from ores in various medium using diverse reducing agents have been comprehensively reviewed by Sinha and Purcell (2019). Carbohydrate based organic reductants such as glucose, sucrose, lactose, sawdust, molasses, corncob and crop wastes are considered effective and environmentally friendly reagents. However, these reductants are yet to find their commercial application due to their expensiveness and high consumption rate in the process whereas limited annual output of renewable carbohydrates are a major concern for them to be used as reducing agents on a commercial scale (Sinha and Purcell, 2019). Organic acids have emerged as both simple and efficient green reductants based on significantly lower oxidation–reduction potential in standard conditions and high Mn recovery. Among various organic acid, the use of oxalic acid (Sahoo et al., 2001; El Hazek and Gabr, 2016), formic acid (Lu et al., 2015), lactic acid (Ma et al., 2015), malonic acid (Lasheen et al., 2014) and citric acid (Godunov et al., 2012) as reducing agents have been investigated for the quantitative recovery of manganese from ores. Ascorbic acid is one such naturally occurring organic acid which is effectively utilized as both reductant and leaching agent for the hydrometallurgical recycling of spent lithium ion batteries and zinc-carbon alkaline batteries (Li et al.,

* Corresponding author.
E-mail address: mksinhajsr@gmail.com (M.K. Sinha).

https://doi.org/10.1016/j.mineng.2020.106406
Received 19 December 2019; Received in revised form 26 March 2020; Accepted 19 April 2020

2012; Nayaka et al., 2015, 2016a, 2016b, 2018, 2019; Chen et al., 2017; Aaltonen et al., 2017; Sayilgan et al., 2010; Kursunoglu and Kaya, 2014). Ascorbic acid has a great ability to absorb molecular oxygen and because of this property, it is considered as a strong reducing agent (Golmohammadzadeh et al., 2018). Ascorbic acid as reductant have never been solely examined for the recovery of manganese form its ores to the best of our knowledge. The present study deals with reductive leaching of ferruginous manganese ore in sulfuric acid medium using ascorbic acid as reducing agent. Effects of various parameters affecting leaching have been investigated in order to determine the optimum conditions for manganese recovery. The leach liquor obtained at the optimized conditions has been used for manganese oxide synthesis. The purity of the manganese oxide synthesized from the purified solution and morphological features have been analyzed by chemical analysis, XRD phase identification and SEM-EDS studies.

2. Experimental

2.1. Materials

The manganese ore was collected from a local mine in South Africa. The chemical analysis of the ferruginous manganese ore is given in Table 1. Prior to the leaching studies, manganese ore was mechanically crushed, ground and screened to 180 μm size. All the chemicals used in the present investigation were of analytical grades and obtained from Merck, India.

2.2. Leaching methodologies

All the leaching experiments were performed in a 500 mL three necked glass reactor placed on a magnetic hot plate equipped with temperature and stirring speed controllers. One neck of the flask was attached with a water condenser while the other two necks were used to insert temperature controller probe and a feed charging/withdrawing of samples during experiment, respectively. Various leaching parameters such as concentration of the leaching reagent, reducing agent dosage, solid/liquid ratio (pulp density), temperature and stirring speed were investigated to optimize the leaching conditions. During leaching, a small amount of the aliquot of leach solution was withdrawn at definite time intervals for analyzing the metal ions concentration using ICP-OES after proper dilution. After completion of the leaching experiment the slurry was filtered to separate leach liquor and leach residue. The leach residues obtained were dried overnight at 353 K in an electric oven and characterized by chemical analysis, XRD and SEM studies (Sinha et al., 2017).

2.3. Purification of leach liquor and synthesis of value added products

In order to remove the ionic impurities from leach liquor obtained at the optimized leaching conditions, the solution was subjected to precipitation at equilibrium pH ~ 6 by adding ammonium hydroxide dropwise under constant magnetic stirring for 60 min. The as obtained precipitate and filtrate was thus analyzed by ICP-OES for the residual metal concentrations. The purified solution of manganese was separately treated with sodium carbonate and oxalic acid to produce manganese carbonate and oxalate respectively. The carbonate and oxalate precipitates were filtered, washed with deionized water three times and dried at 80 °C for 2 h. Finally the manganese carbonate and oxalate powders were calcined in an electrically operated muffle furnace at different temperatures and time periods to produce manganese oxides of different morphologies.

Table 1
Chemical composition of ferruginous manganese ore sample determined by ICP-OES.

Elements	Mn	Fe	Si	K	Ca	Al
Wt.%	25.85	12.35	15.05	0.6	0.4	1.8

2.4. Characterization of the solids

Manganese ore before and after leaching as well as the manganese oxide synthesized in the present investigation were characterized by different techniques such as XRD, SEM-EDX, TG-DTA and chemical analysis as per requirements. X-ray powder diffraction (XRD) patterns (Bruker D8-discover) were obtained with Cu Kα (λ = 1.54178 Å) radiation ranging from 2θ = 10 to 90° at a scanning rate of 2°/min to identify the phases present. The operating voltage and current were kept at 40 kV and 40 mA, respectively. The thermal behavior was investigated in air atmospheres employing thermo-gravimetric (TG) and differential thermal analysis (DTA) equipment (LINSIES GmbH, Germany). The morphologies and particle sizes were also analyzed after sputtering with a conductive layer of iridium, using a field emission scanning electron microscope (JEOL JSM-7800F) with an EDAX attachment for X-Ray microanalysis. The concentrations of metal ions in the ore and the solutions obtained during the leaching and precipitation experiments were determined by using ICP-OES (Prodigy 7-Teledyne Leeman Labs).

3. Results and discussion

3.1. Characterization of manganese ore

Chemical analysis of the manganese ore sample (Table 1) shows the presence of Mn (25.85%), Fe (12.35%) and Si (15.05%) as the major elements while Al, K and Ca respectively are present in minor quantities. The mineralogical phases of manganese ore and its surface morphology were determined by XRD and SEM respectively. The result in Fig. 1 indicates that the manganese ore mainly consists of cryptomelane [$K_{1\text{-}1.5}(Mn^{4+}, Mn^{3+})_8O_{16}$], braunite [$(Mn^{+2}, Mn^{+3})_6SiO_{12}$] and silica ($SiO_2$) along with hematite ($Fe_2O_3$) and pyrolusite ($MnO_2$).

The semi-quantitative XRD analysis of ferruginous manganese ore is presented in Table 2. As can be seen from the SEM (Fig. 2) the morphology of the manganese ore sample is like solid crystalline rock with an uneven surface without substantial porosity. All the peaks obtained in the EDS (energy dispersive X-ray spectroscopy) correspond to Mn, Fe, Si, Al and K. The additional peaks of Ir is due to the iridium coating.

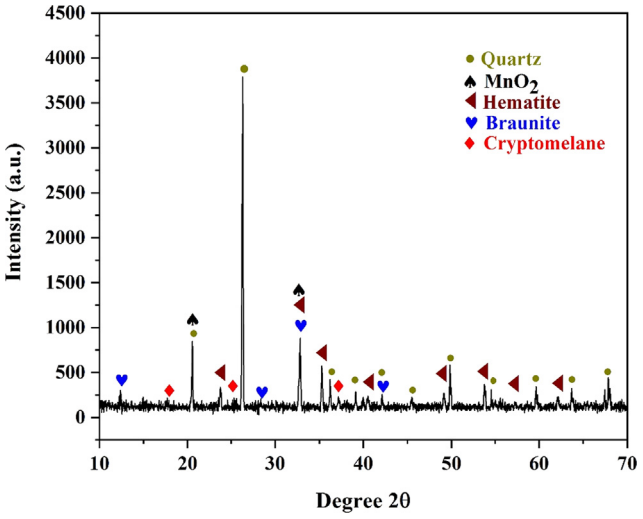

Fig. 1. X-ray diffraction analysis of the manganese ore.

Table 2
Semi-quantitative XRD analysis of ferruginous manganese ore sample.

Phases	Cryptomelane	Braunite	Quartz	Hematite	Mica
Wt.%	14	20	28	25	13

3.2. Leaching of manganese ore using ascorbic acid as a reductant

Preliminary leaching of ferruginous manganese ore have been carried out using 0.5 M H_2SO_4, 100 g/L pulp density and 800 rpm stirring speed in the absence of ascorbic acid as reductant at room temperature for 300 min. It was observed that only ~3% Mn and 2% Fe respectively recovered with 0.5 M sulfuric acid. However when the leaching the manganese ore was carried out by using stoichiometric amount of H_2SO_4 and ascorbic acid (Eq. (1)) at 100 g/L pulp density and stirring speed of 800 rpm, it was observed that ~38% Mn and 8% Fe respectively were leached in 300 min at room temperature (Fig. 3). Since, the recovery of manganese was observed to increase for entire time period, therefore subsequent leaching experiments were performed for a 300 min retention time.

$$10MnO_2 + 10H_2SO_4 + C_6H_8O_6 \rightarrow 10MnSO_4 + 6CO_2 + 14H_2O \quad (1)$$

3.3. Effect of temperature

Since the recovery of manganese was observed to be low at room temperature, the ferruginous manganese ore was leached at 40, 60 and 80 °C in a solution consisting of a stoichiometric amount of H_2SO_4 and ascorbic acid at 100/L pulp density for 300 min to determine the effect of temperature on Mn and Fe leaching. The recovery of both Mn and Fe were found to increase with increase in temperature (Fig. 4). At higher temperature, the viscosity of the solution decreases which accelerates the migration rate of ions, solvent molecules and solid particles, increases the number of collision between molecules, and facilitates the diffusion of leaching agent to ore surface, thus increasing the leaching rate of metal ions (Zhang et al., 2017). At 40 °C dissolution of manganese increased gradually up to 300 min with a maximum leaching efficiency of 43% Mn. When the temperature was raised to 60 °C, within 300 min almost 57% manganese was dissolved in the H_2SO_4 solution along with ~11% of iron. Similar leaching efficiencies have been observed for manganese at both 60 °C and 80 °C (~57% and ~59% Mn respectively). Since ascorbic acid becomes unstable when the temperature is ≤80 °C (Li et al., 2012), therefore a moderate temperature of 60 °C was chosen as the optimum leaching temperature in the current study.

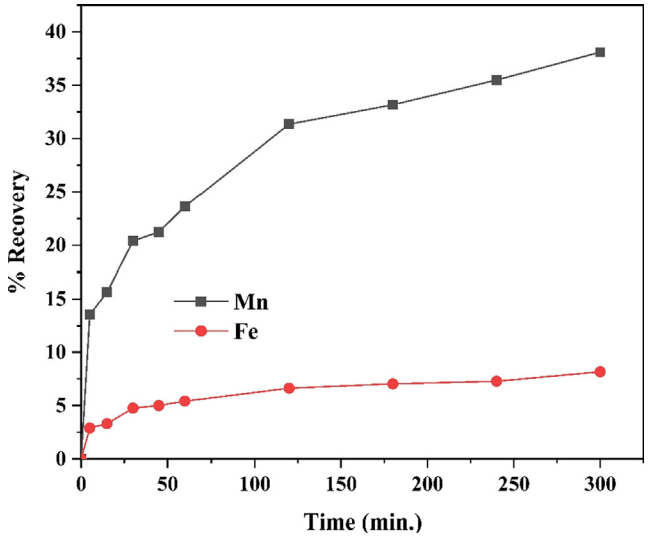

Fig. 3. Leaching of manganese from the ore using a stoichiometric amount of H_2SO_4 and ascorbic acid as reductant. Pulp density: 100 g/L, room temperature, time: 300 min, rpm: 800.

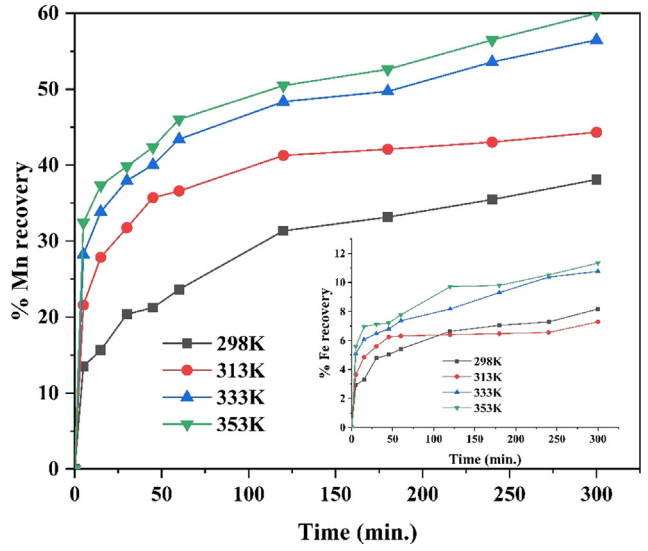

Fig. 4. Leaching of manganese from the ore using a stoichiometric amount of H_2SO_4 and ascorbic acid as reductant. Pulp density: 100 g/L, Temperature: RT-80 °C, time: 300 min, rpm: 800. Inset shows iron leaching at similar conditions.

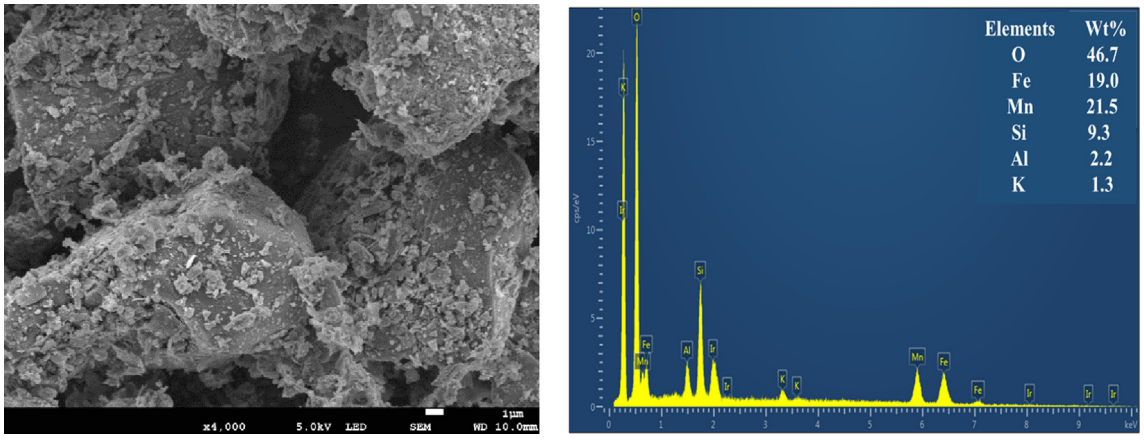

Fig. 2. SEM-EDS of the manganese ore.

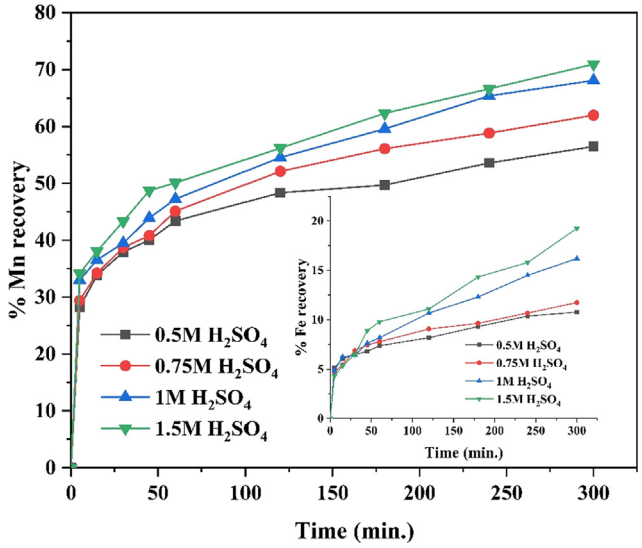

Fig. 5. Leaching of manganese from the ore using stoichiometric amount of and ascorbic acid as reductant. H_2SO_4: 0.5 M −1.5 M, Pulp density: 100 g/L, Temperature: 60 °C, time: 300 min, rpm: 800. Inset shows iron leaching at similar conditions.

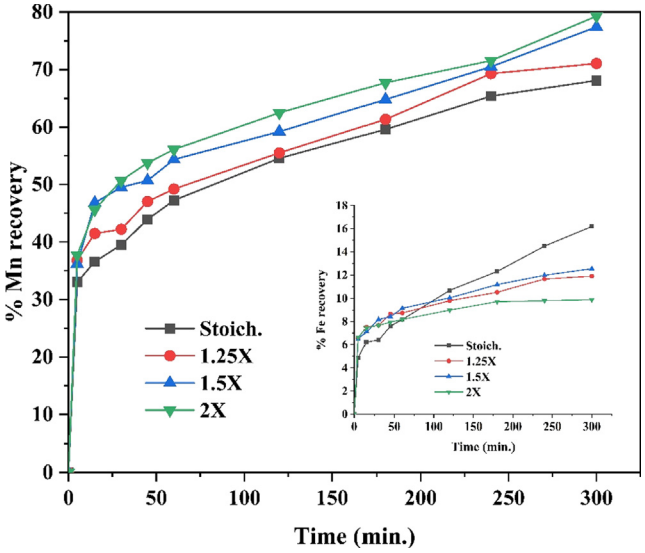

Fig. 6. Leaching of manganese from the ore. H_2SO_4: 1 M, Ascorbic acid: 0.047–0.094 M, Pulp density: 100 g/L, Temperature: 60 °C, time: 300 min, rpm: 800. Inset shows iron leaching at similar conditions.

3.4. Effect of sulphuric acid concentration

The effect of sulfuric acid concentration (0.5–1.5 M) on the leaching efficiency of manganese and iron from the ferruginous manganese ore was studied at 60 °C, 100 g/L pulp density and 800 rpm using stoichiometric amount of ascorbic acid as reductant. Results (Fig. 5) reveal that the leaching of Mn and Fe is strongly affected by the acid concentration and leaching efficiency increases with increase in the H_2SO_4 concentration. It was observed that recovery of manganese increased from ~56% to 71% when using 0.5 M to 1.5 M H_2SO_4. Recovery of iron also exhibits a gradual increase from ~10% to 20% within the same range of acidity. Since the difference in leaching efficiency of Mn while using 1 M H_2SO_4 and 1.5 M H_2SO_4 is approximately 3%, therefore the subsequent experiments were performed with 1 M H_2SO_4 in order to consume less acid for the process and ease in further solution purification.

3.5. Effect of ascorbic acid concentration

For investigating the effect of ascorbic acid concentration, leaching experiments were performed by changing ascorbic acid concentration from 0.047 M to 0.094 M which corresponds to 1–2 times of stoichiometric amount of reductant while keeping other parameters constant i.e. 1 M H_2SO_4, 100 pulp density, leaching temperature of 60 °C and 800 rpm stirring speed for 300 min. It was observed that as ascorbic acid content in the solution increased, the amount of extracted manganese increased as well (Fig. 6). When the ascorbic acid concentration increase from 0.058 M to 0.094 M the recovery of Mn increased from ~71–76% in 300 min while the recovery of iron was observed to be marginally decreased (~12–10%) within the same ascorbic acid concentration. As can be seen the increment in manganese recovery is very small (~2%) between 0.070 M and 0.094 M ascorbic acid concentration, therefore 0.070 M ascorbic acid have been selected for further optimization experiments.

3.6. Effect of agitation speed

Effect of varying agitation speed (400–1000 rpm) was also investigated on the leaching of manganese from the ore with 1 M H_2SO_4, 0.070 M ascorbic acid at 60 °C and 100 g/L pulp density for 300 min. The results obtained are graphically represented in Fig. 7 and revealed

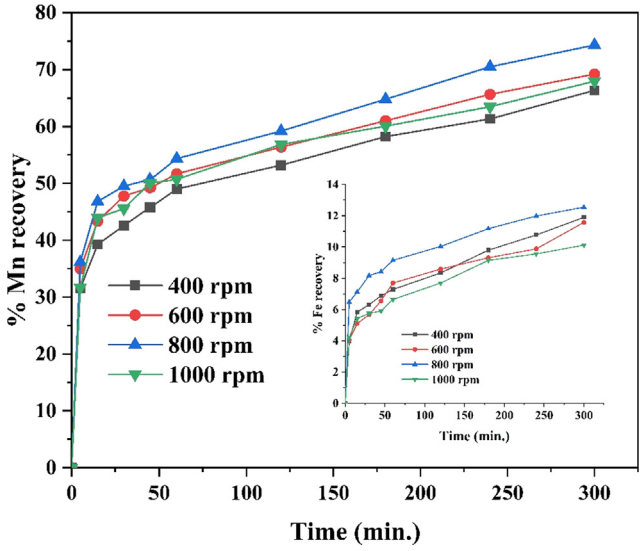

Fig. 7. Leaching of manganese from the ore. H_2SO_4: 1 M, Ascorbic acid: 0.070 M, Pulp density: 100 g/L, Temperature: 60 °C, time: 300 min, rpm: 400–1000. Inset shows iron leaching at similar conditions.

that the leaching ability of manganese was increased from ~67% to 74% with increase in agitation rate from 400 to 800 rpm. A further increase in agitation speed up to 1000 rpm shows antagonistic effect on manganese extraction. The relatively reduced leaching efficiency may be due adherence of ore particles onto the inner wall of three-neck flask because of intense agitation that leads to the worse contact between ore particles and lixiviant. Therefore, the agitation speed was maintained at 800 rpm for further experiments, which was enough to homogeneously suspend the ore particles during leaching. As the difference in manganese recovery with agitation speed is not very large which indicates that that the mass transfer was not much influenced by fluid film around the solid particles, and liquid film diffusion was not the control step of the process (Souza et al., 2007; Nayl et al., 2009). However diffusion of reactants through a solid product layer cannot be ignored.

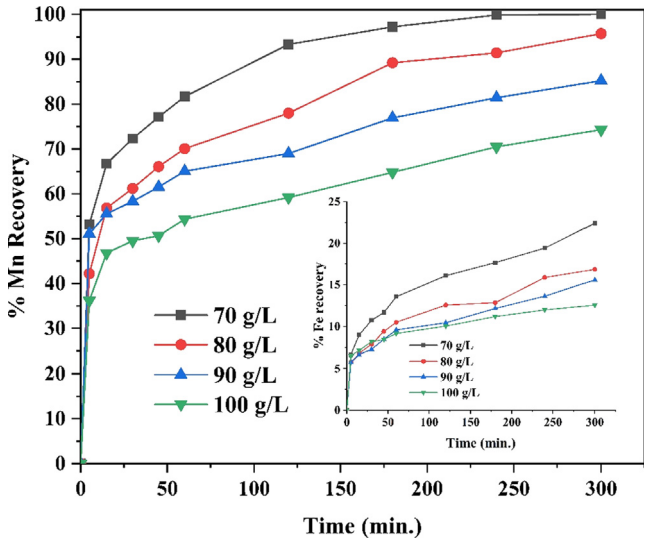

Fig. 8. Leaching of manganese from the ore. H_2SO_4: 1 M, Ascorbic acid: 0.070 M, Pulp density: 70–100 g/L, Temperature: 60 °C, time: 300 min, rpm: 800. Inset shows iron leaching at similar conditions.

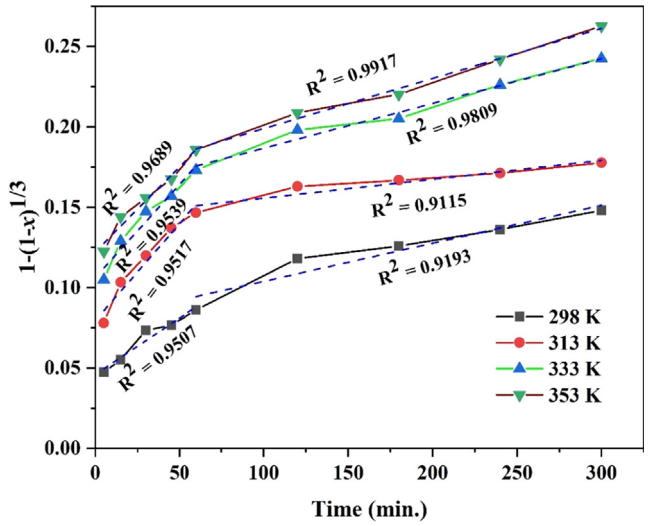

Fig. 9. The chemical controlled kinetic plots for the leaching of manganese.

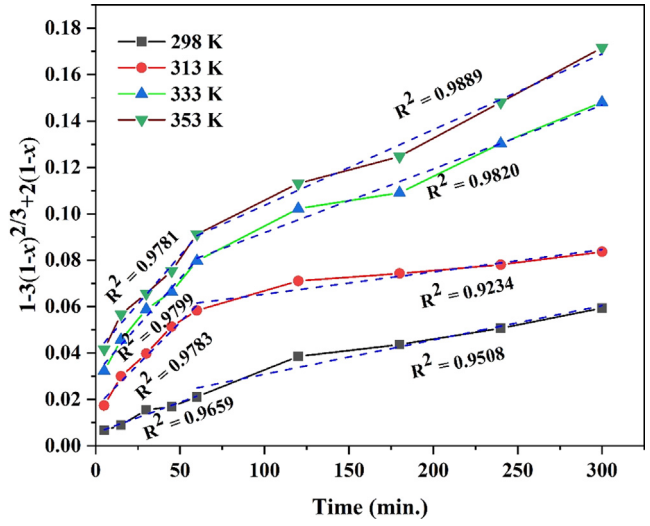

Fig. 10. The diffusion controlled kinetic plots for the leaching of manganese.

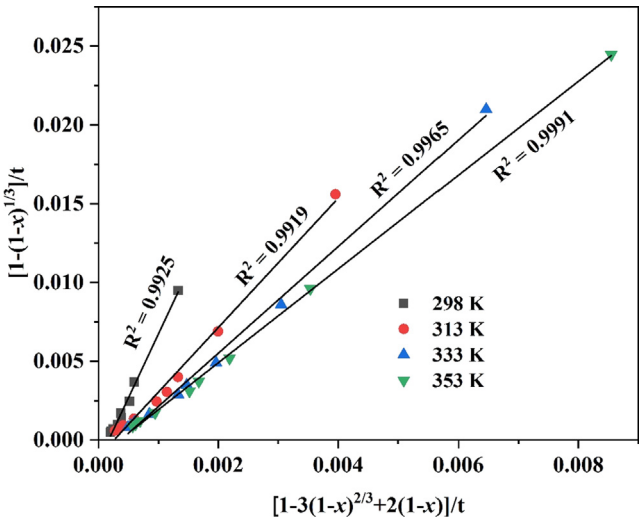

Fig. 11. $\{1 - (1 - x)^{1/3}\}/t$ versus $\{1 - 3(1 - x)^{2/3} + 2(1 - x)\}/t$ plot for manganese leaching from ore.

3.7. Effect of pulp density

The change in the leaching rate and recovery of manganese with changing the solid-to-liquid ratio (pulp density) was investigated using 100 g/L to 70 g/L ratios of the ferruginous manganese ore in 1 M H_2SO_4 leaching solution with 0.070 M ascorbic acid and 800 rpm agitation speed for 300 min. Fig. 8 shows that the rate of leaching and the maximum percentage recovery of manganese increase with decreasing solid–liquid ratio. This shows that decreasing the solid-to-liquid ratio favors a fast mass transfer rate between the ore surface and the sulphuric acid solution. The maximum recovery of manganese increased from ~85% to 96% at a pulp density of 90 g/L and 80 g/L respectively in 300 min leaching time while quantitative (99.9%) recovery of Mn was observed with 1 M H_2SO_4 at a pulp density of 70 g/L. The recovery of iron was also increased with a decrease in pulp density and a maximum of ~22% of Fe recovered at 70 g/L pulp density in 300 min. Since complete leaching of Mn was observed at 70 g/L pulp density, it was considered as the optimum solid-to-liquid ratio for the manganese recovery. It is clear from above studies that the complete recovery of Mn can be obtained by leaching the ferruginous manganese ore with 1 M H_2SO_4 for 300 min at 60 °C and 70 g/L pulp density using 0.070 M ascorbic acid as a reducing agent. The leach liquor obtained under this optimum condition had 18.01 g/L Mn and 1.9 g/L Fe.

3.8. Kinetic analysis

Kinetic investigation was carried out using the data obtained at different temperatures to determine the rate-controlling step and understand the mechanism of manganese leaching from the ferruginous manganese ore. The rate of a reaction in a solid–liquid system can be expressed by heterogeneous models, mainly on the basis of the shrinking core model. According to the shrinking core model, the leaching process is controlled either by the diffusion of the reactant to the solid surface through the solution boundary layer, or through a solid product layer, or by the surface chemical reaction considering the solid as non-porous with a definite shape. As stirring speed had no significant effect on the leaching efficiency of manganese in this study which means that the diffusion of the lixiviant through the solution boundary layer (liquid film) is not the rate controlling step and can be ignored. The following expressions can be used to describe the leaching kinetics of the process for the particles of spherical shape (Levenspiel, 1972):

For chemical controlled leaching kinetics,

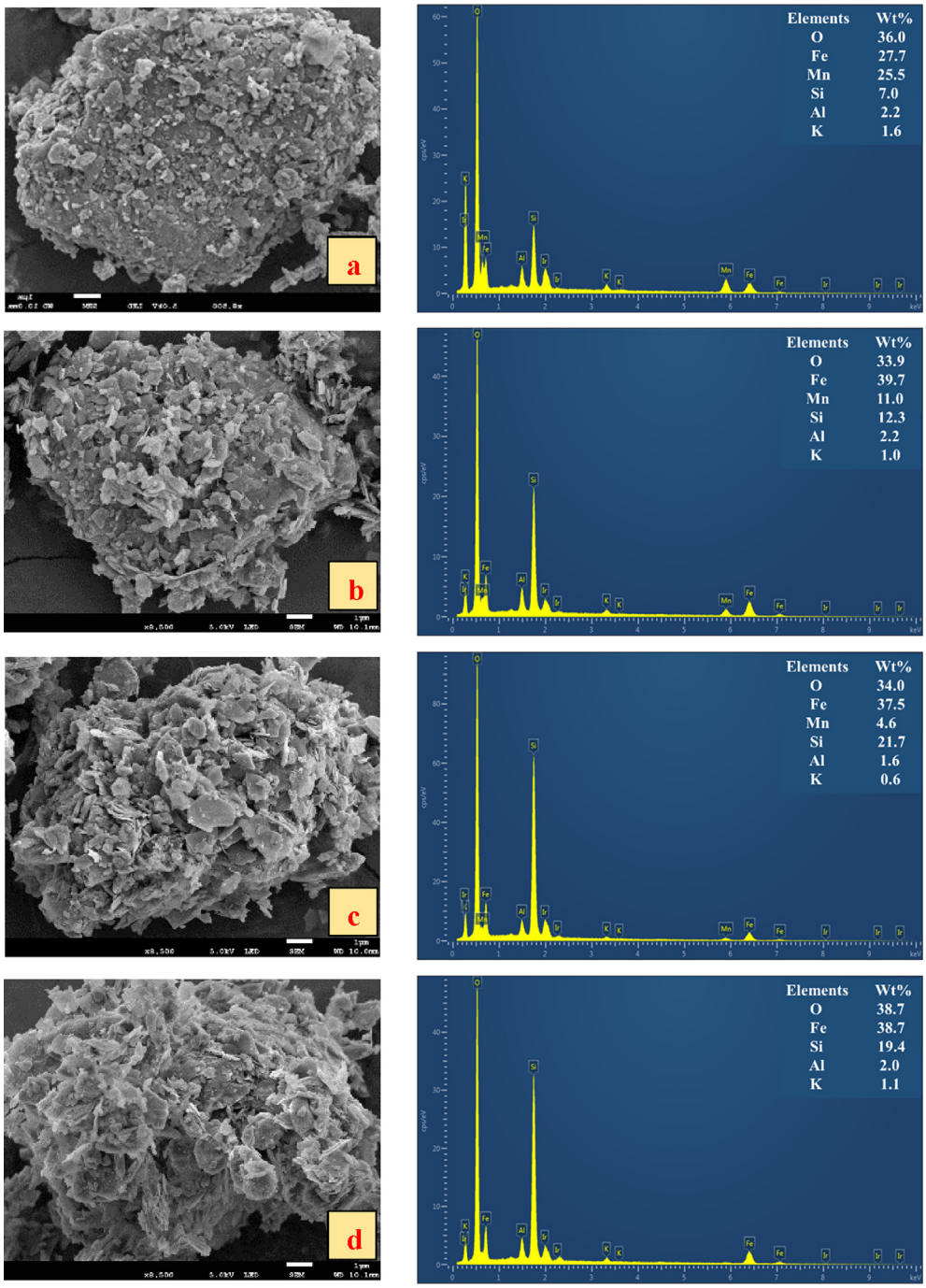

Fig. 12. SEM-EDS images of the leach residues obtained at different leaching time: (a) Mn-ore, (b) 5 min, (c) 60 min and (d) 300 min.

$$1 - (1 - x)^{1/3} = k_c t \quad (2)$$

for leaching kinetic controlled by diffusion through product layer (inert-layer diffusion control),

$$1 - 3(1 - x)^{\frac{2}{3}} + 2(1 - x) = k_d t \quad (3)$$

where x is the fractional conversion of Mn, t is the reaction time (min), k_c and k_d are the specific rate constants (min^{-1}) for chemical controlled and diffusion controlled through product layer respectively.

When the kinetic equations for diffusion through the product layer and the chemical reaction models were applied to the experimental data obtained at different temperatures (Fig. 4), it was observed that that the dissolution rate may not be consistent with one kinetic model throughout the leaching process as parabolic curves were obtained for each model (Figs. 9 and 10). As can be seen from the figures that none of these models really show a good fit and discontinuity have been observed after 60 min of leaching with the change in slope of the straight line which inferred that the leaching of manganese is possibly controlled by a combination of leaching kinetics. Moreover, the linear relationship with high R^2 value (0.99) for the $\{1 - (1 - x)^{1/3}\}/t$ versus $\{1 - 3(1 - x)^{2/3} + 2(1 - x)\}/t$ plot confirms the mixed control leaching kinetics for manganese leaching from ferruginous manganese ore (Fig. 11).

3.9. Characterization of the leached residues

The residues collected at definite time intervals after manganese leaching from the ore under the optimum conditions were examined by

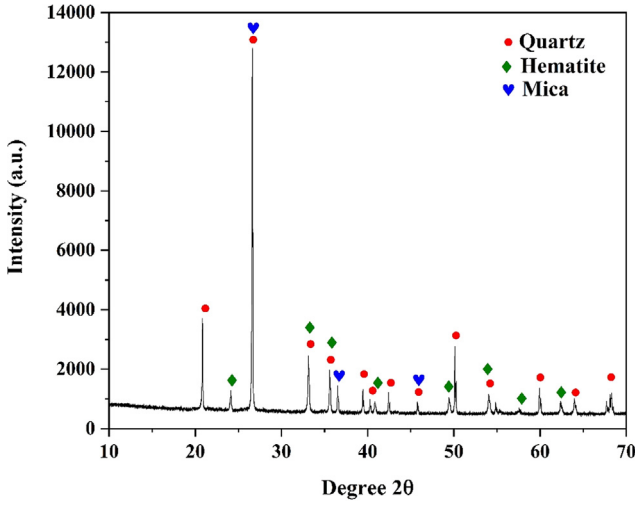

Fig. 13. X-ray diffraction analysis of the final leached residue.

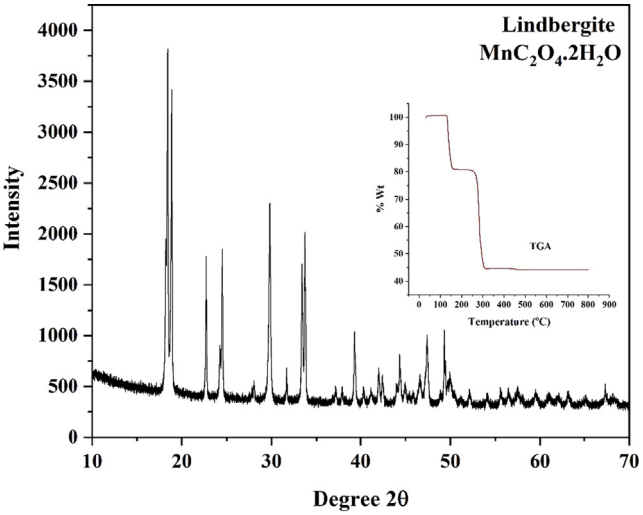

Fig. 14. XRD and TGA curve of as synthesized manganese oxalate.

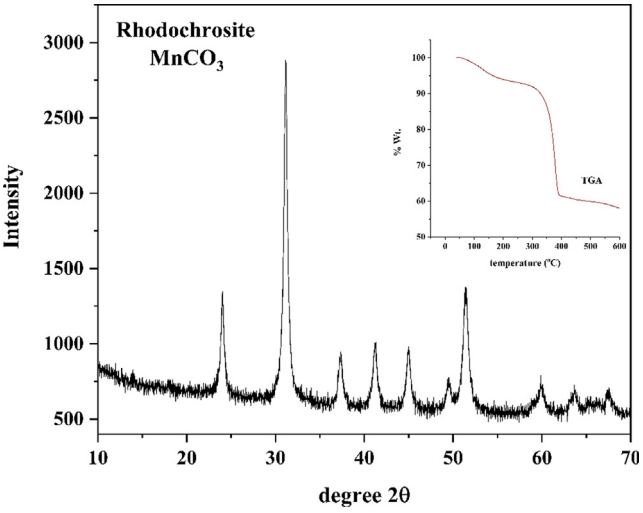

Fig. 15. XRD and TGA curve of as synthesized manganese carbonate.

SEM-EDS and XRD. SEM pictures clearly show that the compact surface of the ore particles becomes corroded and rough as a result of manganese reductive acid leaching and seems to be surrounded by irregular

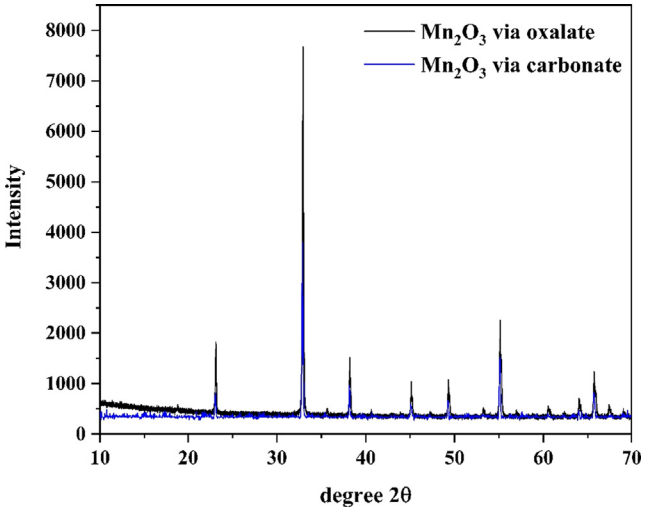

Fig. 16. X-ray diffraction pattern of pure manganese oxide (α-Mn_2O_3).

flakes kind of particles at places which were probably occupied by the manganese complexes before (Fig. 12). As no new product has been formed on manganese dissolution, it is inferred that the insoluble quartz and hematite which are intimately associated with the unreacted surface/core of the ore may act as the inert product layer. The particle size of the material was also not found to decrease to a big extent as the leaching progressed with time which emphasize that leaching is controlled majorly by diffusion of lixiviant through product layer. Energy dispersive X-ray analysis (below SEM image) of leached residues indicates that the manganese content in the leach residues decreased rapidly with time. Leach residues collected after 300 min has shown that Si and Fe are the main products in the residue. X-ray diffraction analysis of the leached residue generated after 300 min reveals the presence of only SiO_2 and Fe_2O_3 as dominant phases (Fig. 13).

The leaching of manganese from ore can be explained first by the chemical dissolution of manganese at the ore surface by reaction between the sulphuric acid and ascorbic acid leading to the formation of the reacted porous layer while SiO_2 and Fe_2O_3 remain adhered in the reacted layer. The next step is the diffusion of the lixiviant through the porous reacted layer surrounded by the inert product layer to the surface of the unreacted core and leading to the dissolution of manganese by chemical reaction at the surface of the unreacted core. Finally, the dissolved manganese diffuses through the solid reacted layer back to the exterior surface of the solid and into the main bulk of the lixiviant. This further suggest that dissolution of manganese from the ferruginous manganese ore was controlled by a mixed controlled leaching kinetics or a combination of chemical reaction and diffusion through the product layer.

3.10. Purification of the leach liquor synthesis of value added products of manganese

It is imperative to further purify the leach solution in order to produce a high-purity Mn product. The quantitative precipitation of iron has been carried out by increasing the pH of the leached solution up to pH ~ 6 using ammonium hydroxide along with small quantity of hydrogen peroxide. After reaching the desired pH the solution kept under constant magnetic stirring for 60 min and then filtered. The purified solution of manganese generated after precipitation was treated with the stoichiometric amounts of oxalic acid and sodium carbonate to produce precipitates of manganese oxalate and manganese carbonate respectively.

The XRD pattern (Fig. 14) of the manganese oxalate so produced matches well with the diffraction peaks indexed for the mineral lindbergite (monoclinic-prismatic manganese oxalate dihydrate);

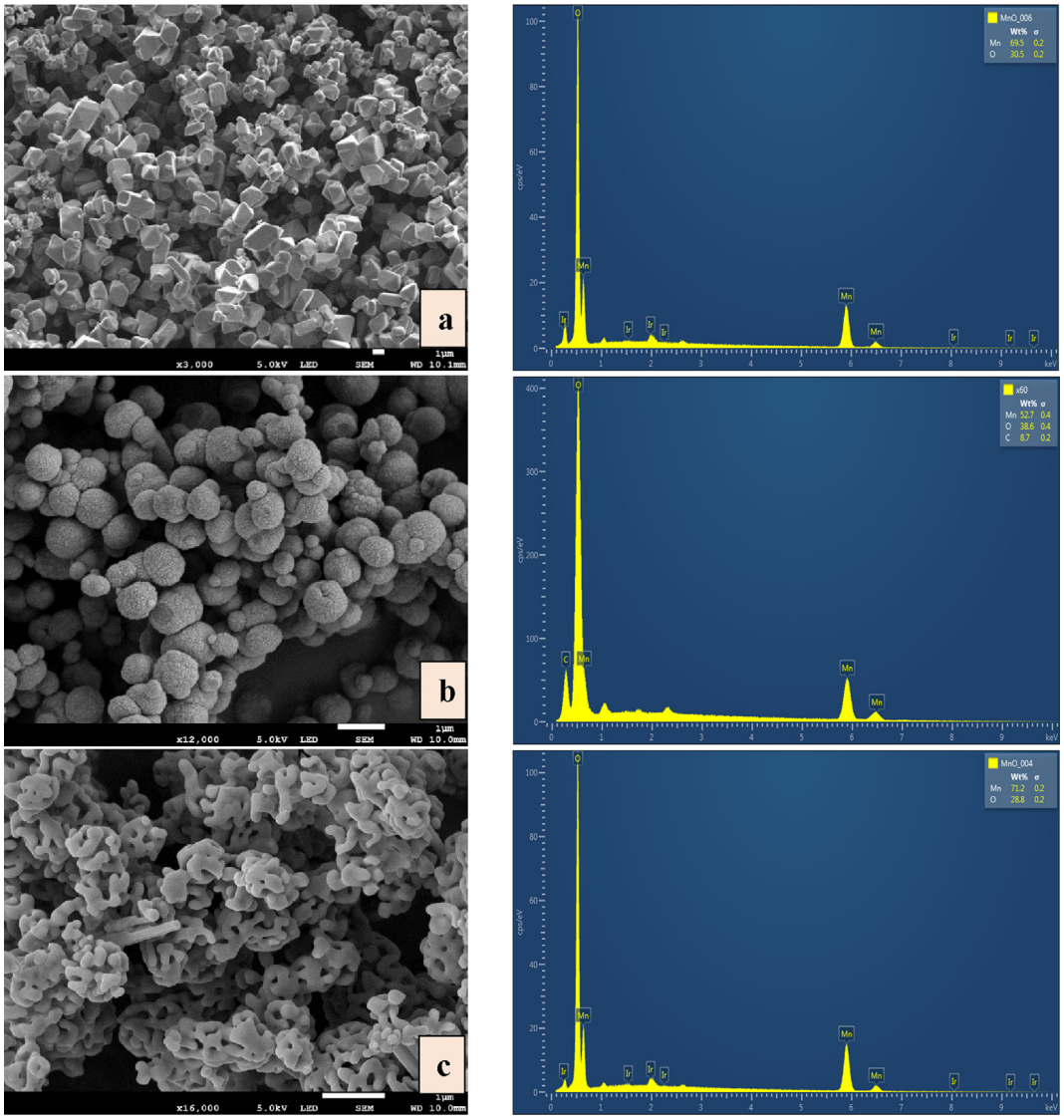

Fig. 17. SEM-EDS of (a) manganese oxide prepared via oxalate route (b) manganese carbonate and (c) manganese oxide prepared via carbonate route.

$MnC_2O_4{\cdot}2H_2O$ Similarly the XRD pattern (Fig. 15) of the manganese carbonate so produced matches well with the diffraction peaks indexed for the mineral rhodochrosite (PDF 44-1472). TGA curve was recorded on heating the above synthesized manganese oxalate up to 800 °C at the heating rate of 10 °C/min in air. Inset of Fig. 14 shows that manganese oxalate decomposes via two weight loss processes *viz.* dehydration to form anhydrous oxalate and decomposition of oxalate to oxide. The first weight loss occurs in the temperature range 115–160 °C with the evaporation of crystallized water, leading to the formation of anhydrous manganese oxalate. Further, the second weight loss region (220–315 °C) accompanied with the decomposition of the anhydrous oxalate and release of CO_2 and CO molecules, is attributed to the synthesis of manganese oxide (Mn_2O_3). The total weight loss of ~55.6% is found to be very close to the theoretical value (55.9%) for the conversion of manganese oxalate dihydrate [$MnC_2O_4.2H_2O$] to manganese sesquioxide (Donkova and Mehandjiev, 2004). Accordingly, the manganese oxalate precursor was calcined at 320 °C for 2 h to convert it completely into manganese oxide.

Similarly, TGA curve of the synthesized manganese carbonate was recorded on heating the above up to 600 °C at the heating rate of 10 °C/min in air. Inset of Fig. 15 shows that manganese carbonate decomposes via two weight loss processes *viz.* dehydration to form anhydrous carbonate and decomposition of carbonate to oxide. The first weight loss occurs in the temperature range 40–250 °C with the evaporation of physically adsorbed water, leading to the formation of anhydrous manganese carbonate. The second weight loss region (250–480 °C) was due to the release of CO_2 by the decomposition of anhydrous $MnCO_3$ and formation of Mn_2O_3 at the same time. The total weight loss of ~31.9% in this region was found to be very close to the theoretical value (31.3%) for the conversion of manganese carbonate to oxide (Mn_2O_3) (Yang et al., 2007, Ashoka et al., 2010). Accordingly, the manganese carbonate was calcined at 500 °C for 6 h to convert it into manganese oxide. The XRD patterns of the as obtained Mn-oxides (Fig. 16) shows that all the diffraction peaks can be indexed as the cubic crystal structure of α-Mn_2O_3 (JCPDS PDF 001-1061). The absence of any oxalate/carbonate phases confirms the complete calcination of the products. Morphology and microstructure of the manganese oxide were also evaluated with SEM as shown in Fig. 17. It is apparent that manganese oxide prepared via oxalate route mainly exists as prismatic particles of ~2 μm size range. However the manganese oxide prepared via carbonate route changes from spherical particles (0.2–1 μm) to porous agglomerated particles, which are more or less spherical and elongated, due to the release of a large amount of CO_2 from the sample.

4. Conclusions

Reductive leaching of manganese from ferruginous manganese ore has been studied by using ascorbic acid as an efficient reducing agent in sulphuric acid medium for the preparation of value added products. Quantitative leaching of manganese is achieved under the optimized condition of 1 M H_2SO_4, 0.070 M ascorbic acid, 60 °C temperature, 70 g/L pulp density, 800 stirring speed and 300 min reaction time. The leaching kinetic of manganese from the ferruginous manganese ore seems to follow the mixed controlled shrinking core model. However, the characterization of leached residue by the XRD and SEM studies further validate the diffusion through the product layer which plays a major role in leaching kinetics of manganese. Iron was completely precipitated from the leach liquor at pH 6 using ammonium hydroxide. From the purified solution of manganese, high pure α-Mn_2O_3 of different morphologies suitable for various applications were prepared by oxalate/carbonate precipitation followed by calcination. The synthesized manganese oxides were characterized by SEM-EDS and XRD.

CRediT authorship contribution statement

Manish Kumar Sinha: Conceptualization, Investigation, Writing - original draft, Writing - review & editing, Validation. **Walter Purcell:** Supervision, Writing - review & editing, Resources. **Willem A. Van Der Westhuizen:** Resources, Writing - review & editing.

Declaration of Competing Interest

The authors declared that there is no conflict of interest.

Acknowledgments

Postdoctoral fellowship provided to Manish Kumar Sinha by University of the Free State, South Africa is highly acknowledged. The authors would like to thank Prof. Langner (Dept. of Chemistry, UFS) for helping in TG analysis. Thanks are also due to Miss Hanlie Grobler (Centre for microscopy, UFS) for her technical assistance in SEM analysis. XRD analysis by Miss Megan W. Purchase (Dept. of geology, UFS) is gratefully acknowledged.

References

Aaltonen, M., Peng, C., Wilson, B., Lundström, M., 2017. Leaching of metals from spent lithium-ion batteries. Recycling 2 (20), 1–9.
Ashoka, S., Chithaiah, P., Tharamani, C.N., Chandrappa, G.T., 2010. Synthesis and characterisation of microstructural α-Mn2O3 materials. J. Exp. Nanosci. 5 (4), 285–293.
Chen, W.S., Liao, C.T., Lin, K.Y., 2017. Recovery zinc and manganese from spent battery powder by hydrometallurgical route. Energy Procedia 107, 167–174.
Donkova, B., Mehandjiev, D., 2004. Mechanism of decomposition of manganese (II) oxalate dihydrate and manganese (II) oxalate trihydrate. Thermochim. Acta 421 (1–2), 141–149.
El Hazek, Gabr, A.A., 2016. Dissolution of manganese from polymetallic material using sulfuric-oxalic acid medium. Am. J. Anal. Chem. 7 (5), 469–477.
Godunov, E.B., Artamonova, I.V., Gorichev, I.G., Lainer, Y.A., 2012. Interaction of manganese (IV) oxide with aqueous solutions of citric and sulfuric acids. Russ. Metall. (Metally) 2012 (1), 39–44.
Golmohammadzadeh, R., Faraji, F., Rashchi, F., 2018. Recovery of lithium and cobalt from spent lithium ion batteries (LIBs) using organic acids as leaching reagents: a review. Resour. Conserv. Recycl. 136, 418–435.
Kursunoglu, S., Kaya, M., 2014. Dissolution and precipitation of zinc and manganese obtained from spent zinc-carbon and alkaline battery powder. Physicochem. Probl. Miner. Process. 50 (1), 41–55.
Lasheen, T.A., Abu Elenein, S.A., Saleh, W.A., Orabi, A.H., Ismaiel, D.A., 2014. Reductive leaching kinetics of low grade manganese deposits in H_2SO_4 solution using malonic acid as reducing agent. Int. J. Sci.: Basic Appl. Res. 15 (1), 151–163.
Levenspiel, O., 1972. Chemical Reaction Engineering. John Wiley & Sons Inc., New York.
Li, L., Lu, J., Ren, Y., Zhang, X.X., Chen, R.J., Wu, F., Amine, K., 2012. Ascorbic-acid-assisted recovery of cobalt and lithium from spent Li-ion batteries. J. Power Sources 218, 21–27.
Liu, B., Zhang, Y., Lu, M., Su, Z., Li, G., Jiang, T., 2019. Extraction and separation of manganese and iron from ferruginous manganese ores: a review. Miner. Eng. 131, 286–303.
Lu, Y., Ma, H., Huang, R., Yuan, A., Huang, Z., Zhou, Z., 2015. Reductive leaching of low-grade pyrolusite with formic acid. Metall. Mater. Trans. B 46 (4), 1709–1715.
Ma, H., Lu, Y., Chen, D., Ming, X., Li, W., Yuan, A., Wei, D.S. Wei., 2015. Reductive leaching of low grade pyrolusite ore with lactic acid. Chin. J. Process. Eng. 15 (6), 976–981.
Nayaka, G.P., Manjanna, J., Pai, K.V., Vadavi, R., Keny, S.J., Tripathi, V.S., 2015. Recovery of valuable metal ions from the spent lithium-ion battery using aqueous mixture of mild organic acids as alternative to mineral acids. Hydrometallurgy 151, 73–77.
Nayaka, G.P., Pai, K.V., Santhosh, G., Manjanna, J., 2016a. Dissolution of cathode active material of spent Li-ion batteries using tartaric acid and ascorbic acid mixture to recover Co. Hydrometallurgy 161, 54–57.
Nayaka, G.P., Pai, K.V., Manjanna, J., Keny, S.J., 2016b. Use of mild organic acid reagents to recover the Co and Li from spent Li-ion batteries. Waste Manage. 51, 234–238.
Nayaka, G.P., Zhang, Y., Dong, P., Wang, D., Pai, K.V., Manjanna, J., Santhosh, G., Duan, J., Zhou, Z., Xiao, J., 2018. Effective and environmentally friendly recycling process designed for LiCoO2 cathode powders of spent Li-ion batteries using mixture of mild organic acids. Waste Manage. 78, 51–57.
Nayaka, G.P., Zhang, Y., Dong, P., Wang, D., Zhou, Z., Duan, J., Li, X., Lin, Y., Meng, Q., Pai, K.V., Manjanna, J., 2019. An environmental friendly attempt to recycle the spent Li-ion battery cathode through organic acid leaching. J. Environ. Chem. Eng. 7 (1).
Nayl, A.A., Awwad, N.S., Aly, H.F., 2009. Kinetics of acid leaching of ilmenite decomposed by KOH: Part 2. Leaching by H2SO4 and C2H2O4. J. Hazard. Mater. 168 (2–3), 793–799.
Sahoo, R.N., Naik, P.K., Das, S.C., 2001. Leaching of manganese from low-grade manganese ore using oxalic acid as reductant in sulphuric acid solution. Hydrometallurgy 62 (3), 157–163.
Sayilgan, E., Kukrer, T., Yigit, N.O., Civelekoglu, G., Kitis, M., 2010. Acidic leaching and precipitation of zinc and manganese from spent battery powders using various reductants. J. Hazard. Mater. 173 (1–3), 137–143.
Sinha, M.K., Pramanik, S., Kumari, A., Sahu, S.K., Prasad, L.B., Jha, M.K., Yoo, K., Pandey, B.D., 2017. Recovery of value added products of Sm and Co from waste SmCo magnet by hydrometallurgical route. Sep. Purif. Technol. 179, 1–12.
Sinha, M.K., Purcell, W., 2019. Reducing agents in the leaching of manganese ores: a comprehensive review. Hydrometallurgy 187, 168–186.
Souza, A.D., Pina, P.S., Leão, V.A., Silva, C.A., Siqueira, P.F., 2007. The leaching kinetics of a zinc sulphide concentrate in acid ferric sulphate. Hydrometallurgy 89 (1–2), 72–81.
Top, S., 2019. Separation of Fe and Mn from manganiferous iron ores via reductive acid leaching followed by magnetic separation. Min. Metall. Explorat. 1–13.
Yang, L.X., Zhu, Y.J., Tong, H., Wang, W.W., 2007. Submicrocubes and highly oriented assemblies of MnCO3 synthesized by ultrasound agitation method and their thermal transformation to nanoporous Mn2O3. Ultrason. Sonochem. 14 (2), 259–265.
Zhang, T., Wang, H., Wang, J., Zhao, P., 2017. Process for reduction leaching Pyrolusite using Hull. IOP Conf. Ser.: Earth Environ. Sci. 94, 1–7.